

# HPLC analysis of PAMAM dendrimer based multifunctional devices

Mohammad T. Islam, Istvan J. Majoros\*, James R. Baker Jr.

*University of Michigan, Center for Biologic Nanotechnology, 200 Zina Pitcher Place, 4027 Kresge II, Ann Arbor, MI 48109, USA*

Received 2 November 2004; accepted 2 May 2005

Available online 13 June 2005

## Abstract

Comprehensive high-performance liquid chromatography (HPLC) analyses were performed on poly(amidoamine) (PAMAM) dendrimer based multifunctional devices. The nanometer-size devices were synthesized by conjugating partially acetylated (Ac) poly(amidoamine) dendrimers of generation 5 (G5) with fluorescein isothiocyanate (FITC), folic acid (FA) and methotrexate (MTX). The devices are intended for targeted intracellular drug delivery to tumor cells through the folate receptor. Methods were developed for detection and separation of various surface functionalized dendrimer conjugates and small molecules (FITC, FA, MTX) using a common gradient. Results indicate that the HPLC technique can be used as a quality control tool for determining purity of the G5 carrier, its acetylated form, and mono-, bi- and tri-functional nanodevices. More importantly, the chromatograms of these novel nanodevices, reported for the first time, provide information on critical properties such as polydispersity, surface heterogeneity and solubility. The benchmark data can be used to optimize the physicochemical properties of the conjugates to improve drug delivery to cancer cells.

© 2005 Published by Elsevier B.V.

*Keywords:* HPLC; PAMAM dendrimer; Multifunctional device; Dendrimer–drug conjugate; Drug delivery

## 1. Introduction

Dendrimers are spherical, well defined, highly branched macromolecules with dense surface functional groups [1–3]. Poly(amidoamine) (PAMAM) dendrimers are methodically constructed from an ethylenediamine (EDA) core through repetitive alkylation and amidation steps in which each iteration yields the next higher generation of the dendrimer [1]. Each alkylation leads to a half generation with multiple terminal methyl ester groups and each amidation results in the synthesis of complete generations with multiple terminal amine functionalities. The controlled synthesis results in well-defined structures with determined molecular masses, which increase as a function of the dendrimer generation. The multivalency of the PAMAM dendrimers along with their relatively monodisperse structure provides a unique platform for a variety of therapeutic and imaging agents [3–8].

In our laboratory, we have developed dendrimer based nanodevices optimized to target complex therapeutics to spe-

cific cancer cells. The device is based on PAMAM dendrimer of generation 5 (G5) having hydrodynamic diameter of about 5.4 nm and theoretically bearing 128 terminal amine groups with theoretical molar mass of 28,826 Da [9]. Folic acid (FA), fluorescein isothiocyanate (FITC), and methotrexate (MTX) were covalently attached to the surface to provide targeting, imaging, and intracellular drug delivery capabilities, respectively. A list of the mono-, bi-, and tri-functional nanodevices is summarized in Table 1. Details of the procedures for synthesis of these devices are described elsewhere [10]. The efficacy of targeted intracellular drug delivery capable of tracking uptake of the material has been described in detail by Quintana et al. [11a], Thomas et al. [11b] and Majoros et al. [12].

In this article, our primary objective is to perform extensive high-performance liquid chromatography (HPLC) characterization of FITC, FA and MTX conjugated G5 dendrimers with various surface functionalities. HPLC is a widely accepted method for separation and purification of small molecules and is widely used in chemical laboratories. Methods were developed to determine a common gradient that can be used to detect small functional molecules (FITC,

\* Corresponding author. Tel.: +1 734 615 0618; fax: +1 734 615 0621.  
E-mail address: majoros@umich.edu (I.J. Majoros).

FA and FITC) and all the mono-, bi- and tri-functional conjugates. The use of a common gradient would allow us to determine the purity of the conjugates (i.e. whether any small molecular impurities are present), and would additionally tell us about the stability of all compounds under the experimental conditions. Since elution of analytes occurs as a result of counter-ion binding and surface interaction between the conjugates and the stationary phase, a great deal of information regarding the surface properties of conjugates can be obtained. To the best of our knowledge, this is the first study involving HPLC characterization to determine the purity and stability of dendrimer-based complex multifunctional devices.

## 2. Experimental

### 2.1. Materials

Ethylenediamine core PAMAM dendrimers of generation 5 were purchased from Dendritech (Midland, MI) in methanol solution (14.17 wt%). Folic acid, fluorescein isothiocyanate, and methotrexate were obtained from Aldrich (St. Louis, MO). Water used in all of the experiments was purified using a Milli-Q Plus 185 water purification system (Millipore, Bedford, MA, USA). The resistivity of the distilled de-ionized water was  $18.2 \text{ M}\Omega \text{ cm}^{-1}$ . The details of the synthesis of the conjugates are described elsewhere [10]. A list of the conjugates along with numbers of terminal groups is summarized in Table 1.

### 2.2. Reversed phase high-performance liquid chromatography (RP-HPLC)

A reversed phase ion-pairing high-performance liquid chromatography system consisting of a System GOLD™ 126 solvent module, a Model 507 autosampler equipped with a 100  $\mu\text{L}$  loop, and a Model 166 UV detector (Beckman Coulter, Fullerton, CA) was used. A Phenomenex (Torrance, CA)

Jupiter 5 $\mu$  C5 silica based HPLC column (250 mm  $\times$  4.6 mm, 300  $\text{\AA}$ ) was used for separation of analytes. Two Phenomenex Widespore C5 guard columns (4 mm  $\times$  3 mm) were also installed upstream of the HPLC column. The mobile phase for elution of different generations of PAMAM dendrimers was a linear gradient beginning with 90:10 water/acetonitrile (ACN) at a flow rate of 1 mL/min, reaching 50:50 after 30 min. Trifluoroacetic acid (TFA) at 0.14 wt% concentration in water as well as in ACN was used as counter-ion to make the dendrimer-conjugate surfaces hydrophobic. The conjugates were dissolved in the mobile phase (90:10 water/ACN). The injection volume in each case was 50  $\mu\text{L}$  with a sample concentration of approximately 1 mg/mL and the detection of eluted samples was performed at 210, 240 or 280 nm. The analysis was performed using Beckman's System GOLD™ *Nouveau* software.

## 3. Results and discussion

Fig. 1 shows the HPLC chromatogram of EDA-core G5 amine terminated PAMAM dendrimer (G5.NH<sub>2</sub>). A linear gradient starting 10% acetonitrile (90% water) and ending 50% ACN (50% water) in 30 min was selected. The method was developed to ensure elution of all the dendrimer conjugates and small molecules (FA, FITC and MTX) from the stationary surface. In addition to detecting impurities, the common method would allow direct comparison among the chromatograms of different conjugates and various surface functionalized dendrimers. A flatter gradient was deliberately chosen so as to expose the surface heterogeneity of all devices within a reasonable amount of time and subject to the condition that all the molecules elute within this time period.

The counter-ion (TFA) concentration used was 0.14 wt% in both aqueous and ACN phases. At this concentration of TFA, the pH of the aqueous solution was  $\sim 2.25$ . The platform for conjugation, G5.NH<sub>2</sub> possesses terminal primary amine as well as tertiary amine groups. Reported titration data of PAMAM dendrimers show two types of protonation events

Table 1  
Mono-, bi- and tri-functional dendrimer conjugates, their terminal groups and functionalities

Sample	Terminal groups <sup>a</sup>	Functionality	Average number of molecules attached <sup>b</sup>
G5.NH <sub>2</sub>	Amine (NH <sub>2</sub> )	Platform	NH <sub>2</sub> —110
G5.NH <sub>2</sub> .Ac	NH <sub>2</sub> , acetamide (Ac)	Platform (surface modified)	NH <sub>2</sub> —28, Ac—82
G5.NH <sub>2</sub> .Ac.FITC	NH <sub>2</sub> , Ac	Mono, imaging (FITC)	NH <sub>2</sub> —24, Ac—82, FITC—4
G5.NH <sub>2</sub> .Ac.FA	NH <sub>2</sub> , Ac	Mono, targeting (FA)	NH <sub>2</sub> —23, Ac—82, FA—5
G5.NH <sub>2</sub> .Ac.FITC.FA	NH <sub>2</sub> , Ac	Bi, imaging (FITC) and targeting (FA)	NH <sub>2</sub> —19, Ac—82, FITC—4, FA—5
G5.Ac.FITC.OH	Ac, hydroxy (OH)	Mono, imaging (FITC)	Ac—82, FITC—4, OH—24
G5.Ac.FA.OH	Ac, OH	Mono, targeting (FA)	Ac—82, FA—5, OH—23
G5.Ac.FITC.FA.OH	Ac, OH	Bi, imaging (FITC) and targeting (FA)	Ac—82, FITC—4, FA—5, OH—19
G5.Ac.FITC.OH.MTX	Ac, OH	Bi, imaging (FITC) and therapeutic (MTX)	Ac—82, FITC—4, OH—19, MTX—5
G5.Ac.FA.OH.MTX	Ac, OH	Bi, targeting (FA) and therapeutic (MTX)	Ac—82, FA—5, OH—18, MTX—5
G5.Ac.FITC.FA.OH.MTX	Ac, OH	Tri, imaging (FITC), targeting (FA) and therapeutic (MTX)	Ac—82, FITC—4, FA—5, OH—14, MTX—5

Abbreviations: FITC—fluorescein isothiocyanate, FA—folic acid, MTX—methotrexate, Ac—acetamide, OH—glycidol; please see Fig. 6 for chemical structure.

<sup>a</sup> Except functional agents FITC, MTX and FA.

<sup>b</sup> Determined from concentration dependent UV measurements [15].

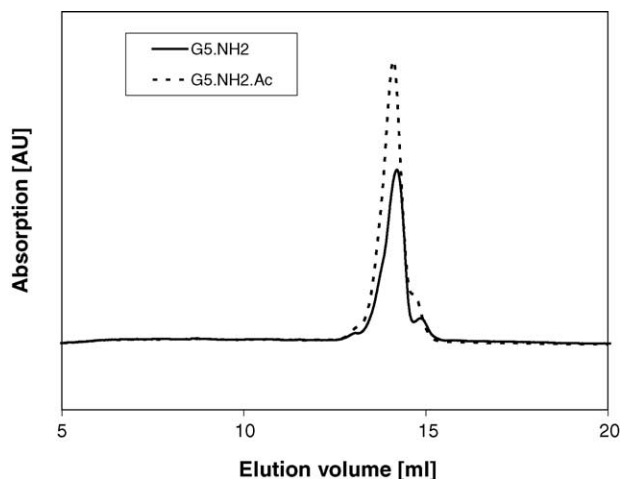


Fig. 1. Chromatograms of amine terminated (G5.NH<sub>2</sub>) and acetylated (G5.NH<sub>2</sub>.Ac) dendrimer platforms.

for the amines. The terminal primary amines have a  $pK$  in the range of 9–10, whereas the interior tertiary amines exhibit a  $pK$  between 4 and 5. At the acidic pH of 2.25, which is well below the two  $pK$  regimes, protonation of both primary and tertiary amines is favored [13].

In contrast to the chromatograms of small molecules, the peak for G5.NH<sub>2</sub> is broad. Besides the main peak, two smaller peaks can also be identified. The broadening of the main peak as well as appearance of smaller peaks can be attributed to the structural defects present during the synthesis of the dendrimer [1]. Occurrences of undesirable side reactions during the successive iterations of alkylation and amidation steps result in macromolecular polydispersity [13]. Some of the structural defects manifest themselves as shoulders or can be embedded in the main peak. A detailed analysis of the structural defects as well as their HPLC profiles can be found elsewhere [13,14].

In sample G5.NH<sub>2</sub>.Ac, about 80% of the cationic amine surface groups are modified to neutral acetamide groups after reacting with acetic anhydride. However, because of the presence of significant primary as well as tertiary amine groups, surface properties do not change appreciably at pH  $\sim$ 2.25 since all surface groups are still protonated. The only noticeable change is the increase in molar absorption coefficient due to the presence of large number of acetamide groups (Fig. 1).

Before discussing chromatograms of conjugated dendrimers, we briefly describe calibrations performed for the functional molecules—FITC, FA and MTX. Each of these molecules have high aromatic contents and are sparingly soluble in water. Considering their limited solubility, the solvent used for dissolving all the small molecules was chosen to be a mixture of 90% water and 10% ACN. Fig. 2 shows the chromatograms for MTX obtained at different concentrations. Since all the chromatograms superimpose onto each other, it can be inferred from this plot that the elution time is independent of concentration at least for the range investigated here. The calibration curve shown in the inset of Fig. 2

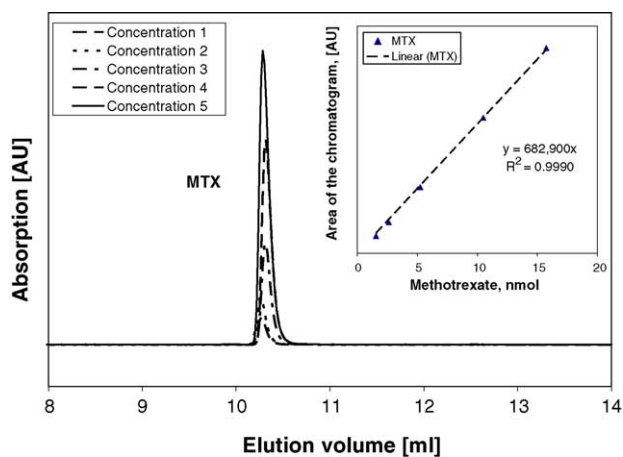


Fig. 2. MTX chromatograms at different concentrations. The inset shows the calibration curve between area under the peak and amount of MTX injected.

shows a linear relationship between the amount of MTX and the area under the peak ( $A_{\text{MTX}} = 682,900 N_{\text{MTX}}$ , here  $A_{\text{MTX}}$  is the area under the chromatogram at 240 nm and  $N_{\text{MTX}}$  is the amount of MTX in nmol) implying negligible intermolecular interaction. It is noteworthy to mention that using the present method it was possible to detect very low ( $\sim$ 1 nmol) amount of MTX. The calibration relation for FA was found to be quadratic,  $A_{\text{FA}} = 1,060 N_{\text{FA}}^2 + 9,180 N_{\text{FA}}$  (correlation coefficient,  $R^2 = 0.9986$ ). For FITC also, the area under the peak is quadratic with respect to the amount of FITC injected [ $A_{\text{FITC}} = 107,640 N_{\text{FITC}}^2 + 187,870 N_{\text{FITC}}$ ,  $R^2 = 0.9978$ ]. The primary factor governing the elution of FA and FITC from the hydrophobic column surface is the density of FA-TFA and FITC-TFA complexes. Since, both FA and FITC are sparingly soluble in the sample solution (90% water and 10% ACN), it is not unlikely that attractive intermolecular interactions between FA or FITC molecules may occur especially at higher concentrations. However, further work is required to validate this viewpoint. In the present work, the individual elution profiles of the functional molecules were obtained only to determine whether there were any unreacted FA, MTX or FITC molecules present after extensive purification of the mono-, bi- and tri-functional nanodevices. Since the multifunctional devices did not exhibit peaks corresponding to free FA or FITC, the complexities of the calibrations due to the presence of quadratic terms were not investigated further.

Conjugation of FA to the acetylated dendrimer through amide linkage (sample: G5.NH<sub>2</sub>.Ac.FA) causes new absorption maximum around 280 nm due to the presence of FA moiety. Because of the presence of aromatic rings, the hydrophobicity of the conjugate increases. However, FA molecules also possess hydrophilic carboxyl ( $-\text{COOH}$ ) and hydroxyl ( $-\text{OH}$ ) functionalities. Therefore, the surface properties and elution time do not change appreciably with conjugation of five (average) moieties present per dendrimer (Fig. 3). The important aspect is that free FA peak was not observed confirming the purity of the mono-functional conjugate.

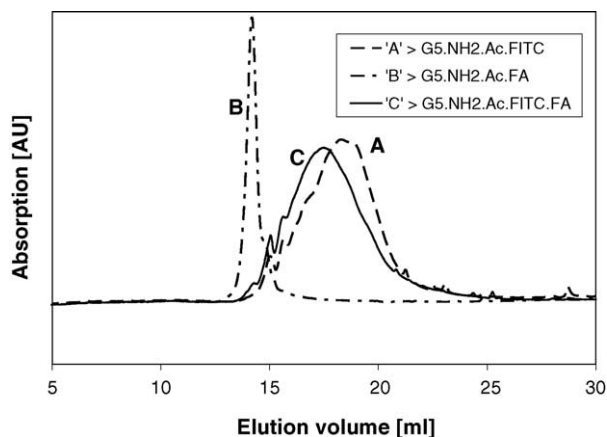


Fig. 3. Elution profiles of FA and FITC conjugated dendrimers.

Due to the presence of four aromatic rings, FITC is the most hydrophobic among the small functional molecules. Conjugation with FITC therefore increases the elution time significantly. This is evident from Fig. 3 where G5.NH<sub>2</sub>.Ac.FITC eluted later as compared to G5.NH<sub>2</sub>.Ac.FA. The fact that the elution time of bi-functional G5.NH<sub>2</sub>.Ac.FITC.FA is intermediate between the elution times of G5.NH<sub>2</sub>.Ac.FA and G5.NH<sub>2</sub>.Ac.FITC also supports this notion.

It is evident from Fig. 3 (as well as from Figs. 4 and 5) that the FITC conjugated G5.NH<sub>2</sub>.Ac.FITC and G5.NH<sub>2</sub>.Ac.FITC.FA devices exhibit broader elution profiles as opposed to the samples that do not contain any FITC molecules. This is due to the fact that FITC is most hydrophobic among the functional molecules. Out of total number of 110 terminal groups of G5.NH<sub>2</sub>.Ac, the functional molecules (FITC, FA, MTX) were attached to only three to five sites. Hence, it can be assumed that in terms of numbers and positions, the functional molecules are statistically distributed. However, in terms of attractions towards the stationary phase, the mismatch in properties between the host platform and the functional molecule is highest for FITC. Therefore, a nan-

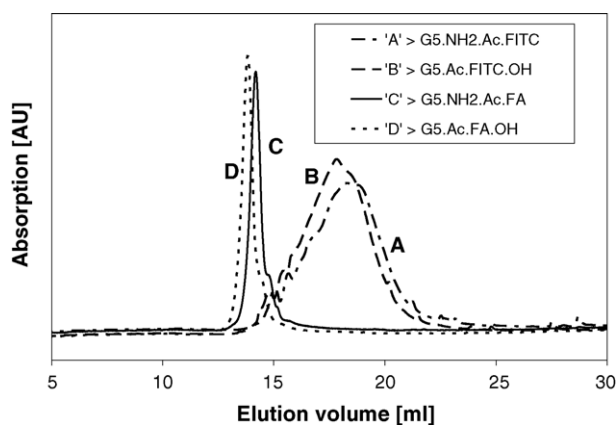


Fig. 4. Comparison between amine and hydroxyl terminated mono-functional (FITC, FA) nano-devices.

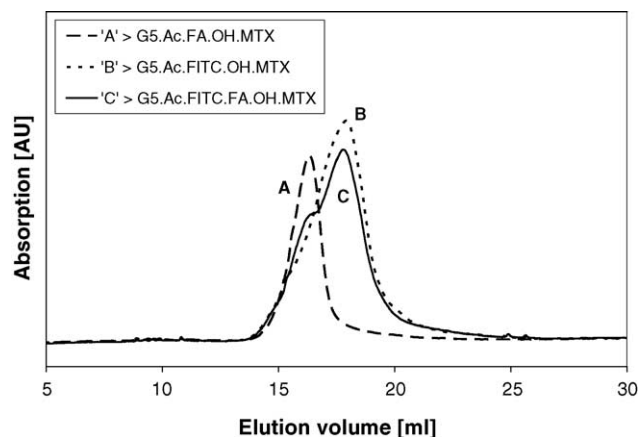


Fig. 5. Chromatograms of MTX conjugated bi- and tri-functional nano-devices.

odevice bearing five FITC molecules is expected to elute much later as opposed to another conjugate having two or three FITC molecules. Hence, statistical distributions of number of FITC molecules would result in broader eluograms as opposed to the distributions of less hydrophobic FA and MTX moieties.

Modification of the remaining amino groups of FA and FITC conjugated dendrimers to hydroxyl end groups by reacting with glycidol is performed to neutralize the terminal amine groups. This is necessary from drug delivery perspective since dendrimers with terminal amino groups can be cytotoxic as cationic amine groups can bind non-specifically with cell surfaces [5]. Also, to optimize drug-delivery, MTX conjugation through ester-linkage requires hydroxyl end groups [10]. From physico-chemical point of view, glycidol terminated dendrimers are more soluble especially at lower pH. Therefore, G5.Ac.FA.OH and G5.Ac.FITC.OH elute faster from the hydrophobic surface of the stationary phase compared to their un-hydroxylated counterparts (Fig. 4). Since hydroxyl termination was performed by reacting with excess glycidol [10], all the amines are expected to be converted to hydroxyl groups. Hence, the breadths of the peaks are expected to remain same which is also found experimentally as displayed in Fig. 4.

The elution profiles of MTX conjugated bi-functional devices (G5.Ac.FITC.OH.MTX and G5.Ac.FA.OH.MTX) are shown in Fig. 5. Purities of the bi-functional devices can be estimated from this plot. Since the purpose of conjugating simultaneously with FA and MTX is to deliver drugs specifically to the cancer cells by targeting through folate receptors, it is important that no free targeting moiety or drug is present [10]. The free drug may non-specifically bind with normal cells in addition to cancer cells thereby killing healthy cells. The peaks corresponding to free MTX or FA cannot be distinguished in Fig. 5, thereby confirming the purity of the conjugate.

The eluogram of the tri-functional device G5.Ac.FITC.FA.OH.MTX exhibits a shoulder in addition to the broad

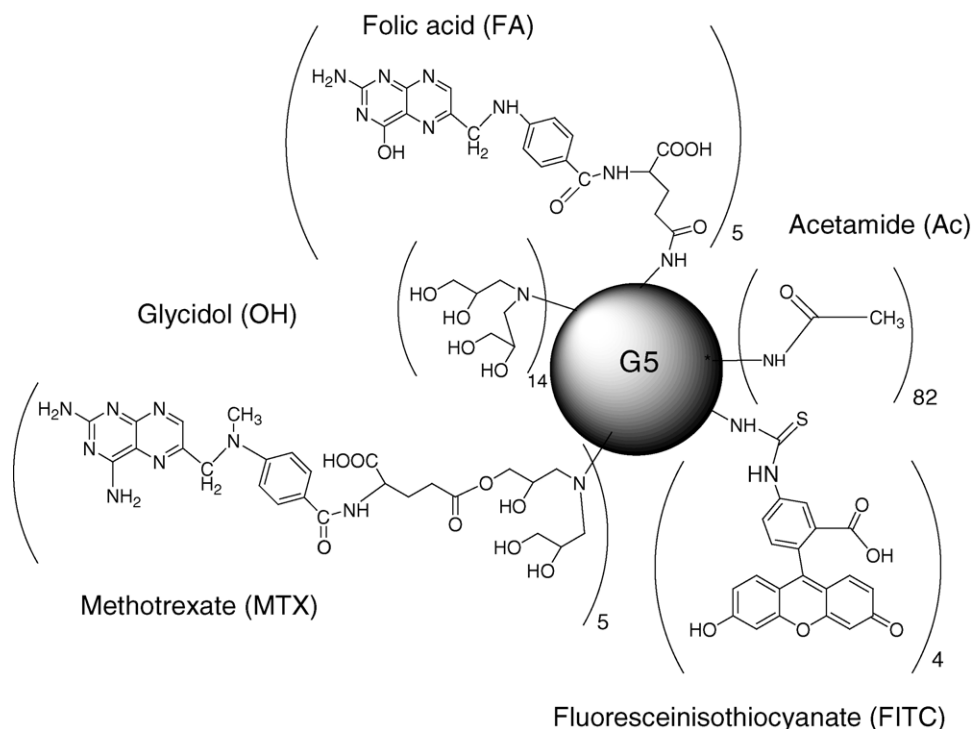


Fig. 6. Structure of tri-functional dendrimer conjugate (G5.Ac.FITC.FA.OH.MTX). The central circle represents EDA-core generation 5 PAMAM dendrimer. Subscripts outside braces indicate approximate average number of small molecules covalently attached to the dendrimer surface.

main peak (Fig. 5). The presence of the shoulder can be explained in terms of the distribution of functional molecules on the dendrimer surface. Both FA and FITC were reacted with the surface modified dendrimer before conjugating with MTX to form the tri-functional device. The average numbers of FA and FITC molecules attached to the dendrimers are five and four, respectively, the distribution of which can be considered statistical following Gaussian, binomial or other mathematical forms. It is possible that the dendrimer molecules bearing less number of FA moieties had more FITC and the macromolecules having more FA functionalities had reacted with less number of FITC, thereby exhibiting bimodal type distribution. This seems to be a reasonable explanation for the presence of the shoulder. In Fig. 5, the elution time of the shoulder is almost equal to the elution time of G5.Ac.FA.OH.MTX thereby suggesting dominance of FA moieties with less number of attached FITC. On the other hand, the peak elution time of G5.Ac.FITC.FA.OH.MTX is similar to the peak elution time of G5.Ac.FITC.OH.MTX implying the predominance of FITC moieties over FA in the main peak.

The surface characteristics of the multifunctional device can be inferred from Fig. 5. MTX conjugation results in delayed elution in case of G5.Ac.FA.OH, whereas earlier elution in case of G5.Ac.FITC.OH suggests that MTX is more hydrophobic than FA but less hydrophobic as compared with FITC. The second observation is readily obvious since FITC contains four aromatic rings. A closer look at the chemical

structures of MTX and FA (Fig. 6) reveal that MTX has one extra methyl group attached to the central 'N' atom and FA has one –OH group instead of –NH<sub>2</sub> attached to the pterin rings. Both the absence of the methyl group and the substitution of –OH in place of –NH<sub>2</sub> make FA more hydrophilic as compared to MTX.

The stability of MTX conjugated nanodevices are of concern since ester linkage is vulnerable depending on the structure of the compound and pH of the medium. Hence, it is important to investigate the stability of the ester bond of the bi and tri-functional devices in comparable physiological conditions which is beyond the scope of the present work. Here,

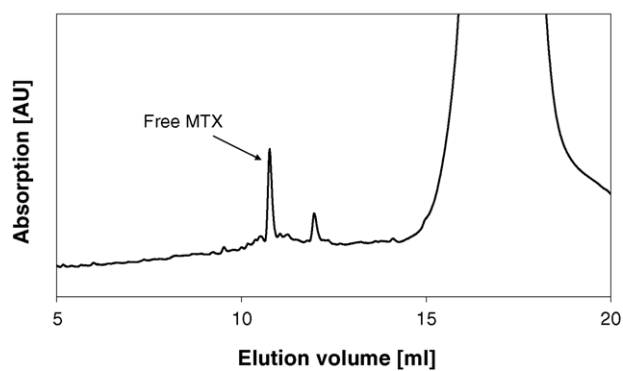


Fig. 7. Eluogram of G5.Ac.FA.OH.MTX after 59 days of incubation at room temperature (22 °C) and in HPLC mobile phase (0.14% TFA in 90% water and 10% ACN).



we analyze the long-term stability of G5.Ac.FA.OH.MTX by aging the sample at room temperature and in the eluent mixture (90% water and 10% ACN) for 59 days. The chromatogram shows an insignificant MTX peak at 10.8 mL. In Fig. 7, we have amplified the ordinate to highlight the MTX peak. The amount of free MTX was estimated using the calibration from Fig. 2. The percentage of free MTX was found to be less than 1% of total MTX confirming the stability of this compound at a pH of 2.25.

### Acknowledgement

This project has been funded by the US National Cancer Institute, National Institutes of Health under contract no. NO1-CO-27173.

### References

- [1] D.A. Tomalia, A.M. Naylor, W.A. Goddard, *Angew. Chem. Int. Ed. Engl.* 29 (1990) 138.
- [2] D.A. Tomalia, H. Baker, J. Dewald, M. Hall, G. Kallos, S. Martin, J. Roeck, J. Ryder, P. Smith, *Polymer J.* 17 (1985) 117.
- [3] R. Esfand, D.A. Tomalia, *Drug Discover Today* 6 (2001) 427.
- [4] S.E. Stiriba, H. Frey, R. Haag, *Angew. Chem. Int. Ed. Engl.* 41 (2002) 1329.
- [5] A.K. Patri, I.J. Majoros, J.R. Baker Jr., *Curr. Opin. Chem. Biol.* 6 (2002) 466.
- [6] K. Kono, M.J. Liu, J.M.J. Frechet, *Bioconjugate Chem.* 10 (1999) 1115.
- [7] P.E. Froehling, H.A.J. Linssen, *Macromolec. Chem. Phys.* 199 (8) (1998) 1691.
- [8] H.M. Brothers II, L.T. Piehler, D.A. Tomalia, *J. Chromatogr. A* 814 (1998) 233.
- [9] P.K. Maiti, T. Cagin, G. Wang, W.A. Goddard, *Macromolecular* 37 (2004) 6236.
- [10] I.J. Majoros, T.P. Thomas, C.B. Mehta, J.R. Baker Jr., *J. Med. Chem.*, in press.
- [11] (a) A. Quintana, E. Raczka, L. Piehler, I. Lee, A. Myc, I.J. Majoros, A.K. Patri, T. Thomas, J. Mule, J.R. Baker Jr., *Pharm. Res.* 19 (2002) 1310;  
(b) T.P. Thomas, I.J. Majoros, A. Kotlyar, J.F. Kukowska-Latallo, A. Bielinska, A. Myc, J.R. Baker Jr., *J. Med. Chem.*, in press.
- [12] I.J. Majoros, T.P. Thomas, J. R. Baker Jr., in: M. Rieth, W. Schommers (Eds.), *Handbook of Theoretical and Computational Nanotechnology*, Chapter 8, in press.
- [13] J. Peterson, V. Allikmaa, J. Subbi, T. Pehk, M. Lopp, *Eur. Polym. J.* 39 (2003) 33.
- [14] M.T. Islam, X. Shi, L. Balogh, J.R. Baker Jr., *Anal. Chem.* 77 (2005) 2063.
- [15] I.J. Majoros, S.R. Gopwani, H.M. Chui, C.B. Mehta, J.R. Baker Jr., submitted for publication.